Supplementary Information for Global predictions of short- to medium-term COVID-19 transmission trends : a retrospective assessment

August 10, 2021

Contents

1 Overview

This supplementary document presents the methods underlying the individual models for the short-term forecasts SI Sec. 2, and updating the reproduction number for the medium-term forecasts to account for population immunity due to infection SI Sec. 3. We also present details of the data and epidemiological parameters used SI Sec. 5 and the criteria for including/excluding a country from the analysis SI Sec. 5.2. Section SI Sec. 4 presents the definitions of the epidemic.

Notation

Hereafter, D_t and C_t represent the number of reported COVID-19 deaths and cases at time t respectively. Since we only used reported deaths to estimate transmissibility, for ease of notation, we drop the superscript D from R_t^D and use R_t to denote the instantaneous reproduction number with respect to deaths at time t. $R[t_1, t_2]$ is the reproduction number between times t_1 and t_2. The most recent estimate of transmissibility is denoted as R_T^{curr}. We use ω to denote the serial interval distribution of deaths i.e. the interval between the deaths of an infectee and their infector, where both the infector and the infectee die. Estimated incidence of deaths at time t is denoted by $\widehat{D}_t$. T refers to last time point in the existing incidence time series of cases or deaths.

2 Methods

2.1 RtI0

The first model relies on a well-established method [1] that assumes the daily incidence of deaths is approximated with a Poisson process following the renewal equation [2]:

$$D_t \sim Poisson\left(R_t \sum_{s=1}^{t} D_{t-s}\omega_s\right) \tag{1}$$

A standard approach to inferring recent transmissibility from an incidence time series relies on the assumption that the effective reproduction number is constant over a window (i.e. the "calibration window") back in time of size τ time units (for example days or weeks) [3]. Adopting a similar approach here, we estimated R_t using only the data in a fixed time-window (of τ days) prior to the most recent observation to calibrate the model. We estimated the average transmissibility $R[T-\tau+1,T]$ over that time-window, but made no assumptions regarding the epidemiological situation or transmissibility prior to this calibration window. Instead, we jointly estimated (using Markov Chain Monte Carlo (MCMC)) combinations of $R[T-\tau+1,T]$ and the incidence of deaths prior to the calibration window $\widehat{D}_t$ for $t = \{1, 2, \ldots T-\tau\}$ that are consistent with the observed deaths in the time window $[T-\tau+1,T]$.

The model likelihood is given by

$$\begin{aligned}
&\mathcal{L}\left(\left\langle \widehat{D}_t \right\rangle, R[T-\tau+1,T] \mid D_{T-\tau+1}, \ldots, D_T\right) \\
&= \prod_{s=T-\tau+1}^{T} P\left(D_s \mid \left\langle \widehat{D}_t \right\rangle, R[T-\tau+1,T], D_{T-\tau+1}, \ldots D_{s-1},\right) \\
&= \prod_{s=T-\tau+1}^{T} Poisson\left(D_s \mid R[T-\tau+1,T] \sum_{k=1}^{s} D_{s-k}\omega_k\right)
\end{aligned} \tag{2}$$

where $\left\langle \hat{D}_t \right\rangle = \{D_1, D_2, \ldots D_{T-\tau}\}$ and $\widehat{D}_t = D_t$ for $t = T-\tau+1, \ldots, T$.

The most recent estimate of transmissibility R_T^{curr} in this model is $R[T-\tau+1,T]$. We then sampled sets of back-calculated early incidence time series $(\widehat{D}_1, \ldots \widehat{D}_{T-\tau})$ and reproduction numbers $(R[T-\tau+1,T])$ from the joint posterior distribution obtained in the estimation process, and projected future incidence $\widehat{D}_{T+i}$ for $i \geq 1$ conditional on these as follows:

$$\widehat{D}_{T+i} \sim Poisson\Bigg(R_T^{curr} \sum_{k=1}^{T+i-1} D_{T+i-k}\omega_k \,|R_T^{curr}, \widehat{D}_1, \dots \widehat{D}_{T-\tau}, D_{T-\tau+1}, \dots D_T, \widehat{D}_{T+1}, \dots, \widehat{D}_{T+i-1}\Bigg), \tag{3}$$

where $\widehat{D}_t = D_t$ for $t = T - \tau + 1, \dots, T$.

During the period covered in the analysis, the epidemiological situation in most countries was changing rapidly with public health measures being reviewed weekly. At the same time, there was a strong 'weekend effect' in the observed data, with typically fewer deaths reported on Saturdays and Sundays. We therefore assumed a fixed calibration window of 10 days to incorporate the rapid dynamics and offset the lower reporting over the weekend. We ran the MCMC for 10000 iterations. We sampled 1000 sets of R_T^{curr} and back-calculated incidence, and for each sampled set, we drew 10 stochastic realisations of the projected incidence of deaths.

2.2 APEestim

Similarly to Model 1, Model 2 relies on the renewal equation (SI Eq. 1) but uses the full time series of observed deaths, and uses information theory to optimise the choice of the calibration window i.e. the time-window of size τ over which $R[T - \tau + 1, T]$ is assumed to be constant in the estimation process [4]. Choices of window size can influence the bias and variance of resulting estimates of transmissibility [5]. We integrated over the entire posterior distribution of R_t (under a given window size), to obtain the posterior predictive distribution of incidence at time $t + 1$ as

$$P\left(D_{t+1} \mid D_1, D_2, \dots D_t\right) = \int_{\mathcal{R}[t-\tau+1,t]} P\left(R_t\right) P\left(D_{t+1} \mid D_1, D_2, \dots D_t, R_t\right) dR_t \tag{4}$$

where $\mathcal{R}[t-\tau+1, t]$ represents the posterior distribution of R_t assuming

a window of length τ. We computed this distribution sequentially for $t \in \{1, 2, \ldots T-1\}$ and then evaluated every observed count of deaths according to their likelihood under the posterior predictive distribution. This allowed us to construct the accumulated predictive error (APE) for a window length τ and under a given serial interval distribution as [4]:

$$APE_\tau = \sum_{t=1}^{T-1} -\log P\left(D_{t+1} \mid D_1, D_2, \ldots D_t\right) \tag{5}$$

Here, D_{t+1} is the observed number of deaths at time $t+1$. The optimal window length τ^* was then chosen as the window for which APE_τ is minimised, optimising the bias-variance trade-off (long windows reduce the estimate variance but increase bias and short windows do the converse).

Again, forward projections were made assuming that transmissibility over the projection horizon remains the same as that in the last τ^* days. That is, R_T^{curr} is set to be $R[T-\tau^*+1, T]$. We then obtain forecasts of deaths as

$$\widehat{D}_{T+i} \sim Poisson\left(R_T^{curr} \sum_{k=1}^{T+i-1} D_{T+i-k}\omega_k \mid D_1, \ldots, D_T, \widehat{D}_{T+1}, \ldots \widehat{D}_{T+i-1}, \right), \tag{6}$$

for $i \geq 1$. We drew 1000 samples from the posterior distribution of R_T^{curr} and for each sampled value, simulated 10 forward trajectories.

2.3 DeCa

Models 1 (RtI0) and 2 (APEestim) use only the time series of deaths to estimate R_t. Model 3 exploits the signal from both the reported deaths and cases to forecast deaths. We assumed that the delay δ between a case being reported and the case dying (for those who die) is distributed according to a gamma distribution with mean μ and standard deviation σ. Let f_Γ be the probability mass function of a discretised gamma distribution.

The cumulative number of reported cases at time t weighted by the delay distribution from case report to death, $\sum_{0}^{\infty} f_\Gamma(x \mid \mu, \sigma) C_{t-x}$, represents the potential number of deaths at time t, if all cases were to die. The ratio ρ_t of the observed number of deaths to this quantity at time t can be thought of as an observed case fatality ratio. We assume that deaths are distributed according to a binomial distribution:

$$D_t \sim Binomial\left(\sum_{0}^{\infty} f_\Gamma(x \mid \mu, \sigma) C_{t-x}, \rho_t\right). \tag{7}$$

The model likelihood is given by

$$\begin{aligned}
&\mathcal{L}\left(\rho_1, \rho_2, \ldots, \rho_T \mid C_1, \ldots, C_T, D_1, D_2 \ldots D_T, \mu, \sigma\right) \\
&= \prod_{s=1}^{T} P\left(D_s \mid C_1, \ldots, C_s, \rho_s, \mu, \sigma\right) \\
&= \prod_{s=1}^{T} Binomial\left(\sum_{0}^{\infty} f_\Gamma(x \mid \mu, \sigma) C_{t-x}, \rho_t \mid C_1, \ldots C_s, \rho s, \mu, \sigma\right).
\end{aligned} \tag{8}$$

We obtained a posterior distribution for $\rho_1, \rho_2, \ldots, \rho_T$ using the conjugate beta prior for ρ_t (using the R package binom [6]), assuming that parameters of the delay distribution μ and σ are known and fixed. The forecasted number of deaths at time $T + i$ for $i \geq 1$ were then drawn from a binomial distribution as

$$\widehat{D}_{T+i} \sim Binomial\left(\sum_{k=0}^{T+i-1} f_\Gamma(k \mid \mu, \sigma) C_{T+i-k}, \rho_T\right). \tag{9}$$

Note that the number of deaths at time $T + i$ depends on the number of cases from the beginning of the epidemic to time $T + i$ for $i \geq 1$. That is, for forecasting deaths at time $T + i$, we need the number of cases at time $t > T$. To augment the observed time series of cases, we assumed that the cases in beyond T are distributed according to a gamma distribution with mean and standard deviation of the observed cases in the last week,

implicitly assuming no growth or decline in cases. We assessed the extent to which this assumption affected our results (SI Sec. 7). Finally, to include transmissibility estimates from this model in the ensemble, we estimated R_T^{curr} using the observed and median forecasted deaths $D_1, \dots D_T, \widehat{D}_{T+i}$ for $i \geq 1$. using the R package EpiEstim [3].

We drew 10000 samples from the posterior distribution of ρ_T and 10000 samples from a gamma distribution to augment the observed cases. We then drew 10000 samples from a binomial distribution (eq. (9)) for each pair of augmented cases trajectory and sampled ρ_T.

2.4 Ensemble Model

We combined the estimates of R_T^{curr}, and the outputs of models RtI0, APEestim, and DeCa into an unweighted ensemble model by sampling the forecasts and reproduction number from each model described above. We also explored building a weighted ensemble by weighting the contribution of each model according to the relative error of the model in the previous week, all previous weeks, across all countries, or estimating the weights independently for each country. We did not find any substantial difference in the performance of the unweighted and weighted ensembles (not shown here). We therefore restricted our analyses to an unweighted ensemble model.

We first drew 10000 samples from the posterior distribution of R_T^{curr} and forecasts from each model and then sampled each posterior distribution with equal weight to build the ensemble posterior distribution of R_T^{curr} and corresponding forecasts.

3 Medium-term forecasts

Accounting for depletion of the susceptible population due to naturally-acquired immunity

As the weighted reproduction number R_t^w already accounts for the population immunity at time t, we first estimated an effective reproduction

number R_t^{eff}, defined as the reproduction number if the entire population were susceptible. That is,

$$R_t^{eff} = \frac{R_t^w}{p_t^S} \tag{10}$$

where R_t^w is the weighted reproduction number at time t and p_t^S is the proportion of population that is susceptible to infection at time t. p_t^S is given by $1 - \sum_{j=0}^{t} I_j/N$ where I_j is the number of infections at time j and N is the total population. In estimating the potential future population immunity using this formulation, we only accounted for naturally acquired immunity assuming that the immunity acquired after infection persists. Since we were forecasting deaths (rather than infections), the true number of infections was estimated using a country-specific age-distribution weighted Infection Fatality Ratio (IFR) (SI Sec. 6).

We then incorporated the effect of a declining proportion of susceptible population due to naturally acquired immunity as

$$R_{t+i}^S = R_t^{eff} p_{t+i}^S \tag{11}$$

From the ensemble estimates of R_T^{curr}, we first estimated R_T^S. The medium-term forecasts were then produced using the renewal equation (SI Eq. 1) and the forecasts used to update the estimates of R_{T+i}^S for each $i \geq 1$ over the forecast horizon.

4 Epidemic Phase

At time t, we defined the epidemic phase in a country to be:

- 'definitely growing' if $R_t^{curr} < 1$ in less than 5% of the samples of the posterior distribution;
- 'likely growing' if $R_t^{curr} < 1$ in less than 20% of the samples of the posterior distribution;

- 'definitely decreasing' if $R_t^{curr} > 1$ in less than 5% of the samples of the posterior distribution;
- 'likely decreasing' if $R_t^{curr} > 1$ in less than 20% of the samples of the posterior distribution;
- 'indeterminate' otherwise.

5 Data and epidemiological parameters

For the weekly analysis, we defined a country as having evidence of active transmission if at least 100 deaths had been reported, and at least ten deaths were observed in each of the past two weeks. Countries with large variability in the reported deaths within each week over the analysis period were excluded from the final analysis for this work (SI Sec. 5.2 lists the full exclusion criterion). Results for 81 countries were included in the work presented here.

We assumed a gamma distributed serial interval with mean 6.48 days and standard deviation of 3.83 days following [7]. For simplicity, we assumed that the delay in reporting a death is the same as the delay from onset to a case being reported. We assumed that the delay in reporting of deaths follows a gamma distribution with mean of 10 days, and standard deviation of 2 days. These figures are roughly consistent with an onset-to-death delay of 15.9 days [8] and onset-to-diagnosis delay of 6.6–6.8 days [9]. The serial interval and delay distributions were discretised using R package EpiEstim [3]. We used a country-specific population-adjusted IFR estimated using the IFR reported in the REACT study (SI Sec. 6).

5.1 Cleaning and pre-processing steps

We used the number of cases and deaths reported by the World Health Organisation (WHO) in the COVID-19 situation report [10]. If either the number of cases or deaths was negative for any country in WHO data, we used the corresponding figures from the data collated by the European

Centre for Disease Prevention and Control [11] (if they were non-negative). If both these sources reported negative numbers, we replaced the negative count on a day with the average of the previous and subsequent 3 days. The deaths time series for each country was then visually inspected and any anomalies (e.g. when a large number of deaths were reported on a single day as a correction) were manually corrected using media reports or alternative sources. A complete list of corrections applied to the data is available on the github repository of this project (`https://github.com/mrc-ide/covid19-forecasts-orderly/blob/main/src/prepare_ecdc_data/prepare_ecdc_data.R`).

5.2 Inclusion/Exclusion Criteria

For the analysis carried out every week, we defined a country as having evidence of active transmission if at least 100 deaths had been reported in a country, and at least ten deaths were observed in the country in each of the past two weeks. Forecasts were produced every Monday for the week ahead (Monday to Sunday) using data reported up to the previous day. Some countries were excluded from the analysis despite meeting these thresholds because the number of deaths per day did not allow reliable inference.

For the summary presented in this manuscript, we included all countries in the weekly analysis except countries with average weekly coefficient of variation (CV i.e. the ratio of standard deviation to the mean) of the reported deaths between 8$^{\text{th}}$ March and 29$^{\text{th}}$ November 2020 greater than 1.1 (the 60$^{\text{th}}$ quantile of the distribution of CV across all countries). This criterion resulted in the exclusion of 53 countries. 81 countries were included in the final analysis.

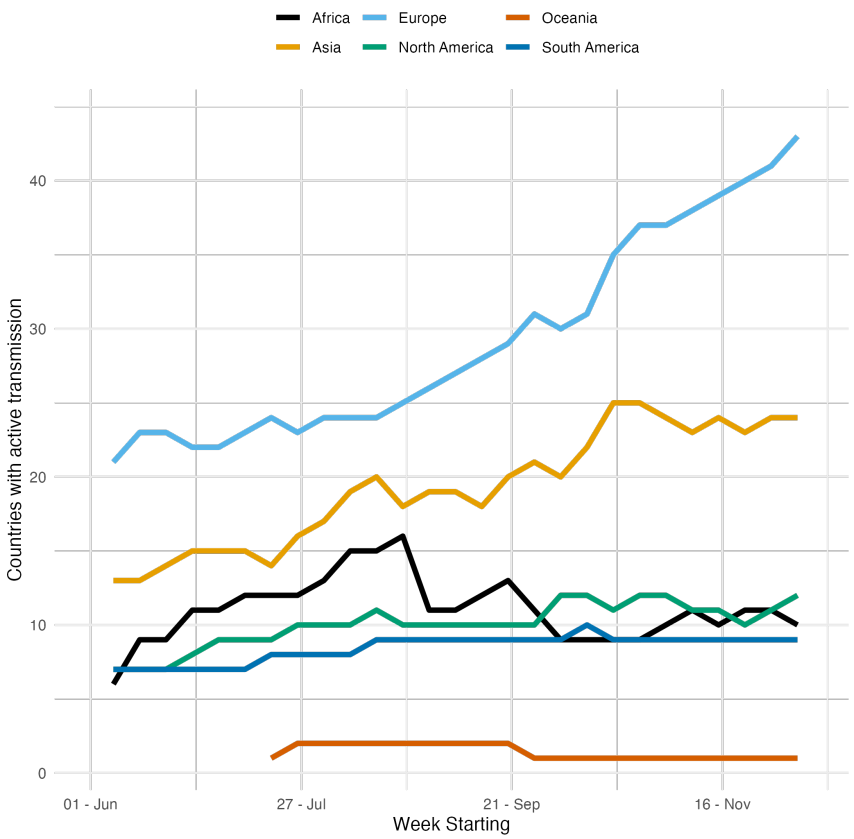

Figure 1. Number of countries included in the weekly reports from 8th March to 29th November 2020. the number of countries included in the weekly analysis grew from 2 in the first week (week starting 8th March 2020), to 94 in the last week of analysis included here (week starting 29th November 2020). Note that some countries that were included in the weekly reports have been excluded from the analysis presented in the manuscript if the average weekly coefficient of variation of the reported deaths between 8th March and 29th November 2020 was greater than 1.1.

6 Infection Fatality Ratio (IFR)

To obtain a IFR distribution, we used the reported deaths and the estimated number of infections in age groups 15-44, 45-64, 65-74 years in the United Kingdom [12]. We first drew 10000 samples from a normal distribution with mean the estimated mean number of infections and standard deviation set to half the width of the 95% CI divided by 1.96. We divided the reported number of deaths in the corresponding age groups by the estimated number of infections to obtain age-disaggregated IFR distributions. We then obtained a country-specific IFR distribution as a weighted sum of the age-disaggregated IFR where the weights are the proportion of the total population in each group in a country [13].

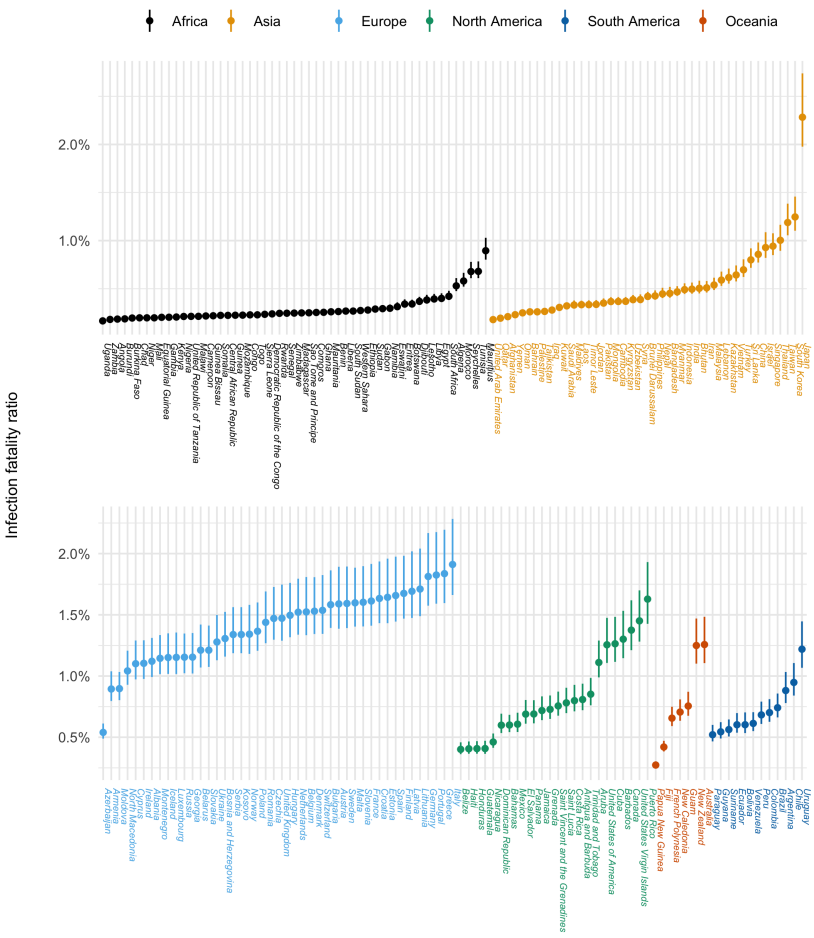

Figure 2. Population adjusted IFR distribution. The solid dots indicate the median estimate and the vertical bars represent the 95% CrI.

7 Augmentation of observed cases for DeCa

In the DeCa model, forecasts of deaths at time t rely on the number of cases from the beginning of the time series to time t. We obtained a distribution of cases in the week for which we are producing forecasts by sampling from a gamma distribution with the mean and standard deviation equal to those of the most recent week of data on cases. We illustrate this process and also show that this does not influence the results under the chosen distribution of delays from case report to death (SI2 Fig. 3).

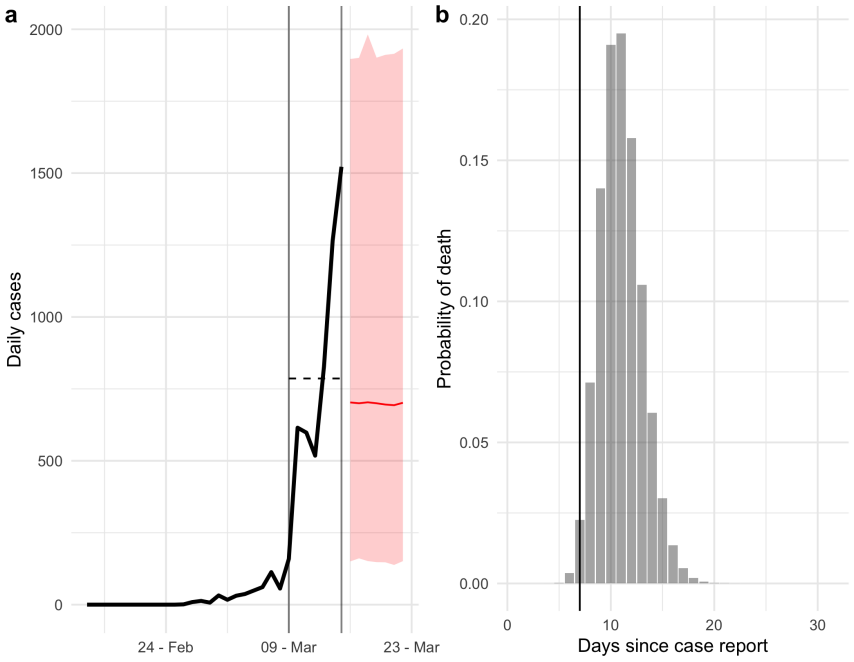

Figure 3. (a) The observed time series of cases (thick black line) is augmented by sampling from a gamma distribution with the mean and standard deviation of the cases in the most recent week of data. The vertical lines indicate the last week and the dashed horizontal line is the mean of the cases in this period. The red line and the shaded area represent the median and the 95% CrI of the sampled cases. (b) The probability distribution of delays from case report to death. For a case reported at time t, the probability of death within d days is the sum of probabilities from 0 to d. In particular, the probability that a case will die within a week (our short-term forecast horizon) is the sum of probabilities to the left of the horizontal line (7 days), which is approximately 2%.

References

[1] Nouvellet P, Cori A, Garske T, Blake IM, Dorigatti I, Hinsley W, et al. A simple approach to measure transmissibility and forecast incidence. Epidemics. 2018;22:29–35. doi:10.1016/j.epidem.2017.02.012.

[2] Fraser C. Estimating individual and household reproduction numbers in an emerging epidemic. PloS One. 2007;2(8). doi:10.1371/journal.pone.0000758.

[3] Cori A, Ferguson NM, Fraser C, Cauchemez S. A new framework and software to estimate time-varying reproduction numbers during epidemics. American Journal of Epidemiology. 2013;178(9):1505–1512. doi:10.1093/aje/kwt133.

[4] Parag KV, Donnelly CA. Using information theory to optimise epidemic models for real-time prediction and estimation. PloS Computational Biology. 2020;16(7):e1007990. doi:10.1371/journal.pcbi.1007990.

[5] Parag KV, Donnelly CA. Adaptive Estimation for Epidemic Renewal and Phylogenetic Skyline Models. Systematic Biology. 2020;69(6):1163–1179. doi:10.1093/sysbio/syaa035.

[6] Dorai-Raj S. binom: Binomial Confidence Intervals For Several Parameterizations; 2014. Available from: `https://CRAN.R-project.org/package=binom`.

[7] Ferguson N, Laydon D, Nedjati Gilani G, Imai N, Ainslie K, Baguelin M, et al. Report 9: Impact of non-pharmaceutical interventions (NPIs) to reduce COVID19 mortality and healthcare demand. 2020;doi:10.25561/77482.

[8] Khalili M, Karamouzian M, Nasiri N, Javadi S, Mirzazadeh A, Sharifi H. Epidemiological characteristics of COVID-19: a systematic review and meta-analysis. Epidemiology and Infection. 2020;148:e130. doi:10.1017/S0950268820001430.

[9] Li M, Chen P, Yuan Q, Song B, Ma J. Transmission characteristics of the COVID-19 outbreak in China: a study driven by data. Epidemiology; 2020. Available from: http://medrxiv.org/lookup/doi/10.1101/2020.02.26.20028431.

[10] WHO Coronavirus Disease (COVID-19) Dashboard; 2021. https://covid19.who.int.

[11] Situation updates on COVID-19; 2021. https://www.ecdc.europa.eu/en/covid-19/situation-updates.

[12] Ward H, Atchison C, Whitaker M, Ainslie KEC, Elliott J, Okell L, et al. SARS-CoV-2 antibody prevalence in England following the first peak of the pandemic. Nature Communications. 2021;12(1):905. doi:10.1038/s41467-021-21237-w.

[13] United Nations, Department of Economic and Social Affairs, Population Division (2019). World Population Prospects 2019.; 2020. https://population.un.org/wpp.